Cell Stem Cell
Article

Notch Signaling Specifies Megakaryocyte Development from Hematopoietic Stem Cells

Thomas Mercher,[1,7,8,*] Melanie G. Cornejo,[1,7] Christopher Sears,[3] Thomas Kindler,[1] Sandra A. Moore,[1] Ivan Maillard,[4] Warren S. Pear,[5] Jon C. Aster,[2] and D. Gary Gilliland[1,6,*]
[1]Department of Medicine, Division of Hematology
[2]Department of Medicine, Division of Pathology
Brigham and Women's Hospital, Harvard Medical School, Boston, MA 20115, USA
[3]Center for Cancer Genome Discovery, Dana-Farber Cancer Institute, Boston, MA 02115, USA
[4]Department of Medicine, Life Sciences Institute and Division of Hematology-Oncology, Center for Stem Cell Biology, University of Michigan, Ann Arbor, MI 48104, USA
[5]Department of Pathology and Laboratory Medicine, Division of Hematology, Abramson Family Research Institute, University of Pennsylvania, Philadelphia, PA 19104, USA
[6]Howard Hughes Medical Institute, Boston, MA 02115, USA
[7]These authors contributed equally to this work
[8]Present address: INSERM EMI0210, Hôpital Necker, Tour Pasteur, 149 Rue de Sèvres, 75743 Paris Cedex 15, France
*Correspondence: tmercher@rics.bwh.harvard.edu (T.M.), ggilliland@rics.bwh.harvard.edu (D.G.G.)
DOI 10.1016/j.stem.2008.07.010

SUMMARY

In the hematopoietic system, Notch signaling specifies T cell lineage fate, in part through negative regulation of B cell and myeloid lineage development. However, we unexpectedly observed the development of megakaryocytes when using heterotypic cocultures of hematopoietic stem cells with OP9 cells expressing Delta-like1, but not with parental OP9 cells. This effect was abrogated by inhibition of Notch signaling either with γ-secretase inhibitors or by expression of the dominant-negative Mastermind-like1. The importance of Notch signaling for megakaryopoietic development in vivo was confirmed by using mutant alleles that either activate or inhibit Notch signaling. These findings indicate that Notch is a positive regulator of megakaryopoiesis and plays a more complex role in cell-fate decisions among myeloid progenitors than previously appreciated.

INTRODUCTION

The Notch signaling pathway is highly conserved among multicellular organisms and has been implicated in a broad range of developmental processes through biological mechanisms that include proliferation, apoptosis, border formation, and cell-fate decisions (Bray, 2006; Wilson and Radtke, 2006). In mammals, there are four single-pass transmembrane Notch receptors (Notch1–4) and five transmembrane ligands (Delta-like [DL]-1/3/4, Jagged-1/2). Most Notch receptor functions are attributable to a canonical signaling pathway that is initiated when the extracellular portion of a Notch receptor binds one of its cognate ligands. This interaction promotes two successive proteolytic cleavages in Notch that are catalyzed first by ADAM family metalloproteases and then by γ-secretase (Schroeter et al., 1998). The latter cleavage releases the intracellular domain of Notch (ICN) from the membrane, allowing it to translocate to the nucleus. In the nucleus, ICN binds to RBPJ (also known as CSL), enabling recruitment of Mastermind-like (MAML) and other critical coactivators, such as p300 or PCAF, that are required for transcriptional activation. The few known direct Notch signaling transcriptional targets include members of the basic helix-loop-helix Hairy enhancer of split (Hes) factors, Hes-related repressor proteins (Herp), Nrarp, Deltex, pre-T cell receptor a, and Gata-3 (Amsen et al., 2007; Fang et al., 2007; Wilson and Radtke, 2006).

In the hematopoietic system, the best-characterized role of Notch signaling is the specific and nonredundant function of Notch1 in T cell over B cell specification and development of T cell progenitors toward the αβ-T cell lineage (Radtke et al., 2004b). Although Notch1-dependent events can be initiated by both DL1 and DL4 in vitro, recent studies suggest that DL4 may be the physiological ligand of Notch1 in vivo (Besseyrias et al., 2007). Conditional inactivation studies have shown that developing thymocytes are dependent on Notch1 until completion of VDJ-β rearrangements at the double-negative (DN)-3 stage. Further maturation of the developing T cells to the DN4 and $CD4^+CD8^+$ double-positive (DP) stages requires attenuation of Notch signaling and coincides with the downregulation of Notch1 (Hasserjian et al., 1996; Huang et al., 2003). Enforced expression of Notch1 at this transitional stage interferes with positive selection and development of CD4 or CD8 single-positive T cells (Visan et al., 2006). The importance of stage-specific regulation of Notch activation during T cell development is underscored by Notch mutations associated with malignant transformation of the T cell lineage (Weng et al., 2004). More than 50% of patients with T cell acute lymphoblastic leukemia bear activating Notch1 receptor mutations localized within the heterodimerization domain and/or the PEST domain, which regulates protein stability of the receptor. Apart from its well-established role in lymphopoiesis, the role of Notch signaling on other aspects of hematopoiesis, including hematopoietic stem cell (HSC) self-renewal and myeloid differentiation, has been controversial (de Pooter et al., 2006; Mancini et al., 2005; Stier et al.,

2002; Wilson and Radtke, 2006). However, the available evidence generally supports the notion that Notch not only negatively regulates B cell lineage but also myeloid lineage development as a concomitant of its role in supporting T cell-fate decisions.

Megakaryopoiesis is the mechanism by which HSCs differentiate into mature megakaryocytes that ultimately produce platelets, critical for hemostasis in the peripheral blood vasculature. The megakaryocytic lineage is thought to derive directly from a common bipotent megakaryocyte-erythrocyte progenitor (MEP) (Akashi et al., 2000; Debili et al., 1996). However, it remains controversial whether MEPs arise from a committed common myeloid progenitor (CMP) (Akashi et al., 2000), directly from a very primitive uncommitted HSC (Adolfsson et al., 2005; Forsberg et al., 2006), or from both developmental pathways. The thrombopoietin receptor (*MPL*) and its ligand, thrombopoietin (*TPO*), are essential for the proliferation of megakaryocyte progenitors and their differentiation into mature platelet-producing megakaryocytes (Goldfarb, 2007; Kaushansky, 2005). However, although megakaryocyte numbers are markedly reduced in *MPL*-deficient mice, these animals still produce both megakaryocytes and platelets, indicating that HSCs are capable of fate decisions that result in megakaryopoiesis in the absence of MPL. Several transcription factors, including *GATA-1*, *GATA-2*, *FOG1/ZFPM1*, *RUNX1*, and *NFE2*, are important for normal megakaryopoiesis, but among the hematopoietic transcription factors expressed by erythroid and megakaryocytic lineages, no single factor has been identified that exclusively specifies megakaryocytic fate (Goldfarb, 2007). Therefore, a unifying mechanism controlling these different transcription factors as they cooperate to engage megakaryocytic cell fate remains to be elucidated. In this report, we demonstrate a previously unappreciated role for Notch signaling as a positive regulator of megakaryocyte fate.

RESULTS

The DL1/Notch Axis Induces Megakaryocyte Differentiation of LSK In Vitro

Murine bone marrow $Lin^{-}Sca\text{-}1^{+}cKit^{+}$ (LSK) cells were cocultured, in the absence of exogenous cytokines, on OP9-GFP cells or OP9 cells expressing the Notch ligand Delta-like1 (OP9-DL1) (Schmitt et al., 2004; Schmitt and Zuniga-Pflucker, 2002) (see Figure S1 available online). Phase-contrast microscopy showed that LSK cells cultured on OP9-DL1 cells, but not OP9-GFP, gave rise to large cells with cytoplasmic protrusions reminiscent of proplatelet production by megakaryocytes (Figure 1A). The megakaryocytic nature of these cells was confirmed by Wright-Giemsa and acetylcholinesterase (AchE) staining that demonstrated large $AchE^{+}$ cells with multilobated nuclei in OP9-DL1, but not OP9-GFP cocultures (Figure 1A and Figure S2B). Flow cytometric analyses showed that LSK cells cocultured with OP9-DL1 gave rise to a transient population of $CD41^{+}Ter119^{+}$ DP cells after 5 days (Figure S2A) and to a population of $CD41^{+}Ter119^{-}$ (Figures 1B and 1C) cells by day 8 of coculture, whereas few $CD41^{-}Ter119^{+}$ or $CD41^{-}Mac1^{+}$ cells were detected. In contrast, LSK cells cocultured with OP9-GFP differentiated into both $CD41^{-}Ter119^{+}$ erythroid cells and $CD41^{-}Mac1^{hi}$ granulocyte-macrophage cells (Figures 1B and 1C). Additional evidence for enhanced megakaryopoiesis in LSK/OP9-DL1 cocultures compared to LSK/OP9-GFP cocultures included an elevated number of $CD41^{+}CD42b^{+}$ megakaryocytes and an increased median ploidy (Figures S2C and S2D) as well as an increased capacity to form megakaryocyte colonies (CFU-Mk) after replating in methylcellulose or collagen-based semisolid cultures (Figures S3). We next tested the effect of coculturing human hematopoietic cells with OP9-DL1. As was observed for the murine LSK cells, flow cytometric analysis of human bone marrow $CD34^{+}$ cells cultured on OP9-DL1 stroma showed increased numbers of $CD41^{+}$ cells and decreased numbers of $Mac1^{+}$ cells compared to cells cultured on OP9-GFP (data not shown). Together, these results indicate that in vitro stimulation of murine LSK or human $CD34^{+}$ cells with DL1 suppresses granulocyte-macrophage and erythroid differentiation but promotes megakaryocytic maturation. The observation of a transient $CD41^{+}Ter119^{+}$ DP population (Figure S2A) further suggests that megakaryocytes observed at day 8 of coculture may arise from a progenitor with combined erythroid and megakaryocytic potential.

Canonical Notch Pathway Mediates Megakaryocyte Fate

To confirm that Notch signaling was the basis for induction of megakaryocyte development by OP9-DL1 stroma, we first treated the cocultures with Compound E or DAPT, two γ-secretase inhibitors that prevent cleavage of the Notch receptors and pathway activation (De Smedt et al., 2005; Weng et al., 2004). The increase in megakaryocyte differentiation upon coculture of LSK cells with OP9-DL1 cells was abrogated by addition of either these inhibitors (Figure 1D and data not shown). These findings indicate that pharmacologic agents selectively inhibiting the Notch pathway abrogate megakaryocytic and restore granulocyte-macrophage differentiation of LSK cells cultured on OP9-DL1 cells.

We next tested the role of Notch-mediated transcriptional activation in megakaryopoiesis. We utilized a dominant-negative MAML1 mutant (dnMAML1), fused to GFP, that entraps all four mammalian intracellular Notch (ICN1–4) in transcriptionally inert RBPJ/ICN/dnMAML1 complexes (Nam et al., 2006; Weng et al., 2003) and is therefore a potent inhibitor of Notch-mediated transcription. LSK cells transduced with dnMAML1 prior to the initiation of cocultures with OP9-DL1 failed to differentiate into $CD41^{+}$ cells (Figure 2A). Conversely, expression of ICN1 or ICN4 in LSK cells cultured on OP9-GFP stroma was sufficient to induce megakaryopoiesis in the absence of DL1 stimulation, with a marked increase in $CD41^{+}$ cells (Figure 2B). Retroviral transduction and expression of the Notch targets, Hes1 or Hes5, in LSK cells partially recapitulated megakaryocyte differentiation on OP9-GFP stroma in the absence of DL1 stimulation (Figure 2B). Importantly, ICN4 expression rescued the inhibition of megakaryocyte development by γ-secretase inhibitor on OP9-DL1 stroma (Figure 2C). Taken together, these results indicate that activation of the RBPJ/ICN/MAML complex in the LSK compartment mediates megakaryocytic fate determination in vitro.

Notch Signaling Initiates a Megakaryopoietic Transcriptional Program

To gain insight into the molecular basis for the DL1-induced megakaryopoiesis, we first assessed expression of the Notch target Hes-1 (Jarriault et al., 1995) by quantitative RT-PCR

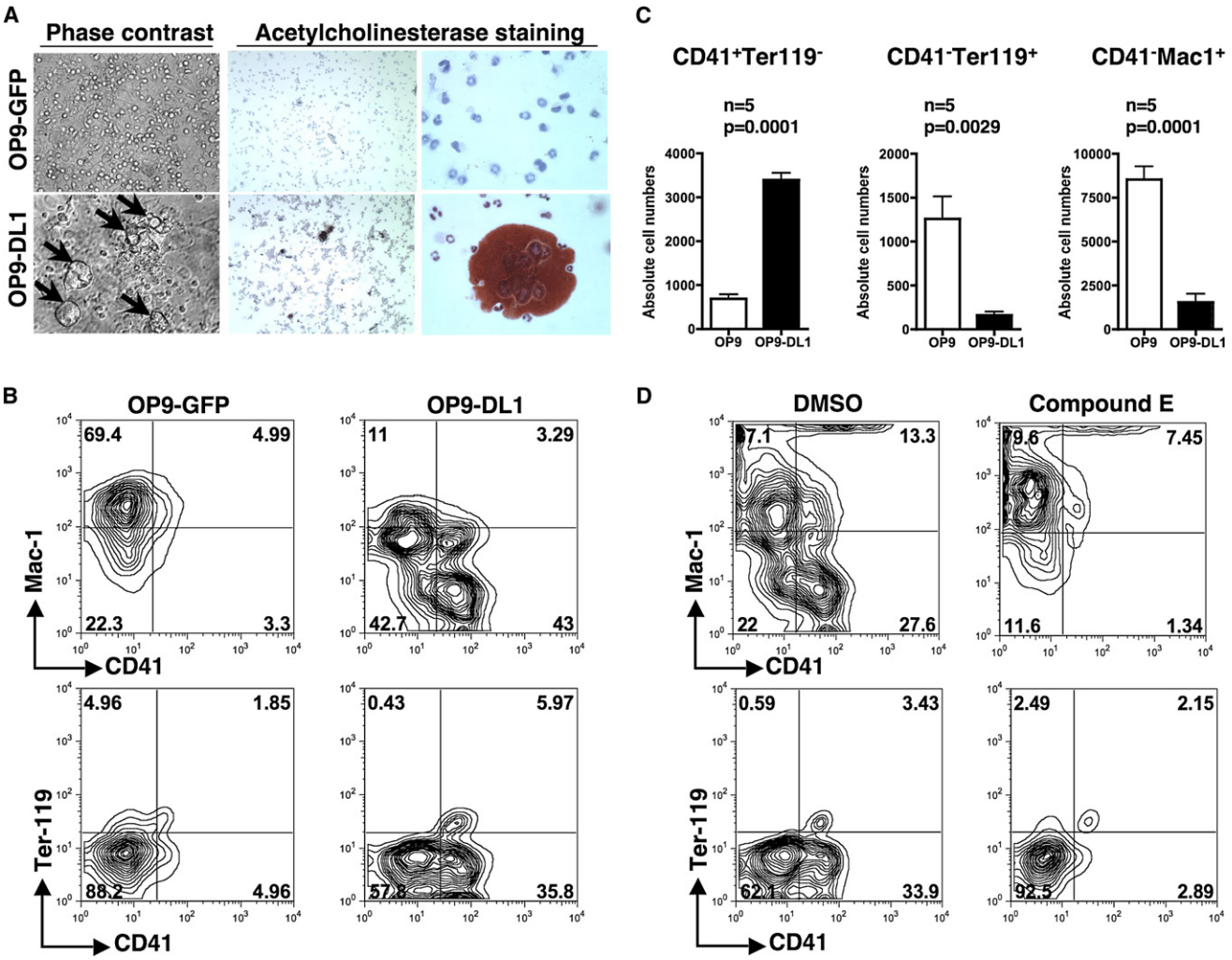

Figure 1. The DL1/Notch Axis Induces Megakaryocyte Differentiation In Vitro

(A) Flow-sorted LSK cells were plated on OP9-GFP or OP9-DL1 stroma. (Left panels) Phase-contrast microscopy of day 8 LSK cells/OP9-GFP or OP9-DL1 stroma cocultures. Arrowheads indicate megakaryocytes observed in OP9-DL1 cocultures. Original magnification is ×400. (Middle and right panels) Acetylcholinesterase (AchE) staining of cytospun cells from cocultures. Original magnification was ×100 and ×600, respectively. Brown coloring indicates positivity for AchE.

(B) Flow cytometric analysis of $CD45^+$ cells derived from day 8 LSK/OP9-GFP or OP9-DL1 cocultures.

(C) Histogram representation of flow cytometric results presented in (B). Mean ± SEM of five independent flow cytometric analyses after 8 days of coculture is shown.

(D) γ-secretase inhibition abrogates biological and molecular effects of DL1 stimulation. LSK cells cultured on OP9-DL1 stroma in the presence of DMSO (control) or Compound E (CompE, 1 μM) were analyzed for megakaryocytic differentiation.

analysis. LSK-derived cells obtained after 5 days of coculture with OP9-DL1 showed a 50-fold increase in expression of Hes-1 compared to cells derived from OP9-GFP cocultures, an effect that was also abrogated by addition of Compound E (Figure 3A). Furthermore, expression of GATA-1 and Fli-1, two transcription factors that are required for normal megakaryopoiesis (Deveaux et al., 1996), was also increased in cells cultured on OP9-DL1 compared to OP9-GFP stroma. Conversely, expression of PU.1, a transcription factor that is essential for normal myeloid development and antagonizes GATA-1 (Nerlov et al., 2000; Rekhtman et al., 1999; Zhang et al., 1999), showed decreased expression in LSK cocultures with OP9-DL1 compared to OP9-GFP stroma (Figure 3A).

To have a comprehensive view of the transcriptional changes associated with Notch-induced megakaryocyte development, we performed global gene expression array analysis of LSK cells cultured for 3 days on OP9-GFP, OP9-DL1, or OP9-DL1 supplemented with Compound E, respectively. We generated two lists of genes implicated in the Notch signaling pathway or in megakaryopoiesis (Notch and Megakaryocyte Gene Lists, respectively, Tables S1 and S2) and performed gene set enrichment analysis (GSEA) (Krivtsov et al., 2006; Subramanian et al., 2005), a computational method that determines whether a defined gene set shows differential expression between two biological states. When comparing LSK/OP9-GFP and LSK/OP9-DL1 coculture conditions, we observed a significant enrichment of

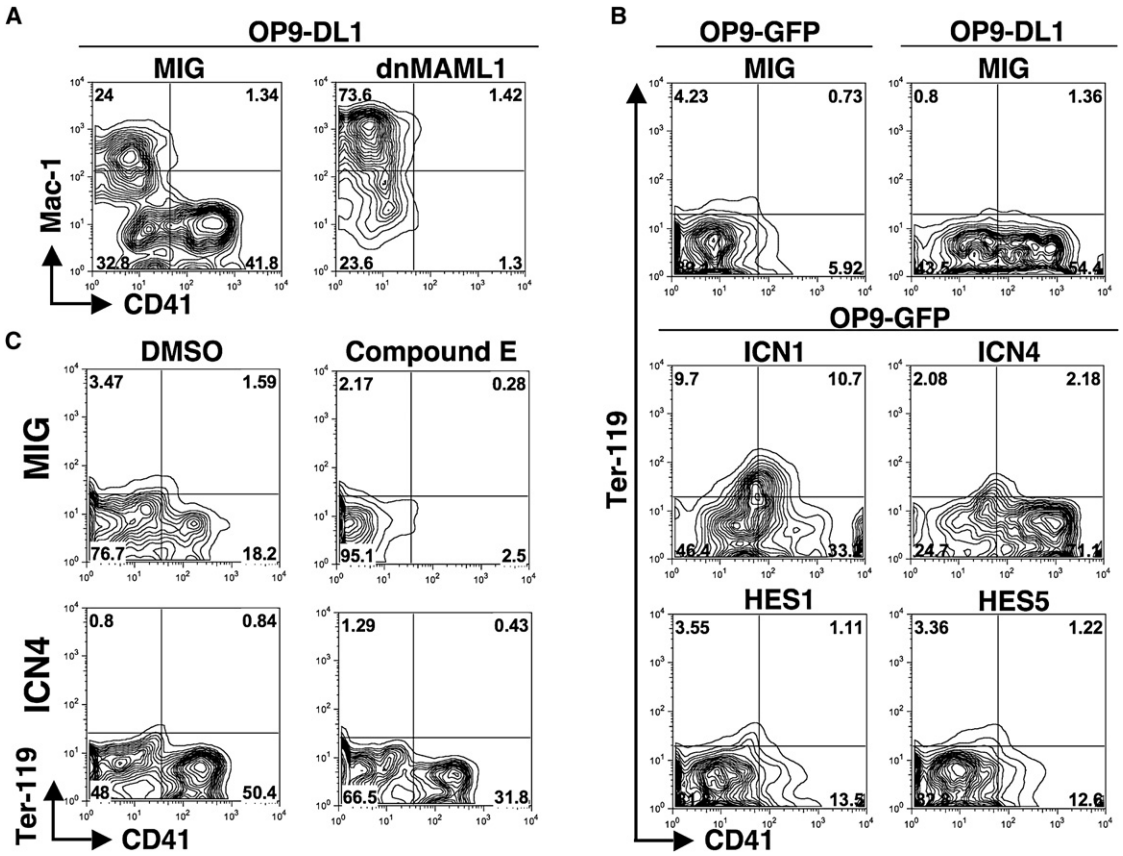

Figure 2. RBPJ/ICN/MAML Complex Mediates Megakaryocyte Development

(A and B) LSK cells were transduced with retroviruses encoding either dnMAML1, ICN1, ICN4, HES1, HES5, or MIG-empty vector control and subsequently plated on OP9-GFP or OP9-DL1 stroma.

(C) LSK cells were transduced as in (A) and (B) and plated in presence of 1 μM Compound E or mock (DMSO) control. FACS analyses of $CD45^+GFP^+$ cells were performed after 8 days of coculture.

Notch target genes in the latter condition, consistent with activation of the Notch pathway by DL1 (Figures S4A and S4B). We also observed significant enrichment in megakaryocyte-specific genes when comparing the LSK/OP9-DL1 with LSK/OP9-GFP coculture conditions (Figures 3B and 3C). The "leading edge" genes, the subset of the Megakaryocyte Gene List that accounts for the enrichment, included those encoding transcription factors (e.g., *GATA-1*, *GATA-2*, *FOG1/ZFPM1*, *NFE2*), cytokine receptors (e.g., *MPL*, *IL1R*, *KIT*, *PDGFRb*), and structural or granule proteins (e.g., *ITGA2B*, *ITGB3*, *GP1BA*, *CD9*, *VWF*). In contrast, the expression of the leading edge genes derived from the Megakaryocyte Gene List was not increased when Compound E was added to the LSK cells/OP9-DL1 cocultures (Figures 3C and 3D). Taken together, these findings indicate that DL1-stimulated LSK cells engage a transcriptional program characteristic of both Notch pathway activation and megakaryocyte development.

Notch Specifies Megakaryocyte Fate at Several Levels of HSC Differentiation

To measure the frequency of LSK cells that can develop into megakaryocytes, individual wells of 96-well plates coated with either OP9-GFP or OP9-DL1 stroma were seeded with 1, 2, 5, or 20 LSK cells. Assessment of megakaryocyte development after 8 days of culture indicated that about 1 in 12 LSK cells can give rise to megakaryocytes on OP9-DL1 stroma compared to an estimated 1 in 360 on OP9-GFP stroma (Figure 4A). To determine which subpopulation of LSK cells is the most efficient for megakaryocyte development, we fractionated LSK cells (Adolfsson et al., 2005; Forsberg et al., 2006; Pronk et al., 2007), based on their expression of Flt3 and CD34, into long-term HSC ($Flt3^-CD34^-$LSK cells), short-term HSCs ($Flt3^-CD34^+$LSK cells), and lymphoid-primed multipotent progenitors ($Flt3^+CD34^+$LSK) and plated them in OP9-GFP and OP9-DL1 cocultures (Figure 4B). Differentiation toward $CD41^+$ cells was more important when LT- and ST-HSCs were plated on OP9-DL1, compared to LMPP. Of note, LT- and ST-HSCs also showed an increased differentiation toward erythroid and megakaryocytic lineages when cultured with OP9-GFP stroma. Together, these results suggest that Notch stimulation favors megakaryocyte differentiation of LSK cells at the single-cell level, and although all LSK subpopulations can differentiate into megakaryocytes upon Notch stimulation, LT- and ST-HSC appear more efficient at this process compared to LMPP.

To investigate the role of Notch on more committed myeloid progenitors in vivo, we first analyzed quantitative expression of

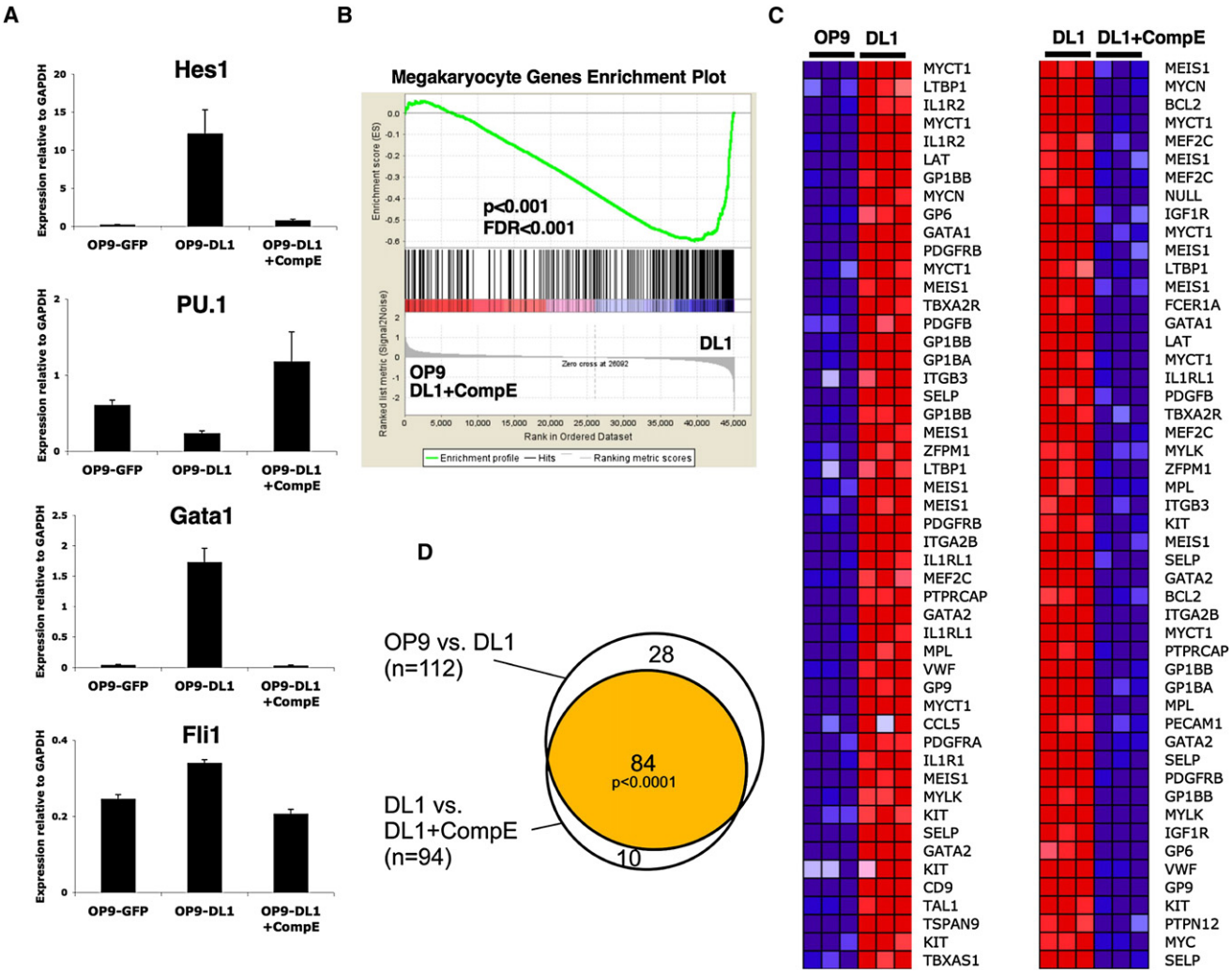

Figure 3. Notch Activates a Megakaryocyte-Specific Transcriptional Program in LSK Cells

(A) RNA from LSK cells cocultured with OP9-GFP or OP9-DL1 in the presence or absence of Compound E (1 μM) for 5 days was used to perform analysis of Hes-1, Gata-1, Fli-1, and PU.1 expression normalized to Gapdh. Mean ± SEM of duplicate experiments is represented.

(B) Flow-sorted LSK cells were cultured on stroma (OP9-GFP, OP9-DL1, or OP9-DL1 supplemented with 1 μM Compound E). After 3 days of cocultures, RNA from nonadherent cells was extracted, amplified, labeled, and hybridized on mouse 430.2E Affymetrix chips. Expression data were analyzed for a list of genes positively involved in megakaryopoiesis by using GSEA. Enrichment plot showing upregulation of megakaryocyte-specific genes in OP9-DL1 versus OP9-GFP and OP9-DL1+Compound E. P value and FDR are indicated.

(C) Heat map representation of the expression of the top 50 megakaryocyte leading edge genes enriched in OP9-DL1 cultures compared to OP9 and OP9-DL1 supplemented with inhibitor cultures.

(D) Venn diagram representation of megakaryocytic genes induced by Notch pathway activation in LSK cells.

Notch receptors on various myeloid progenitor populations purified by flow cytometry (Figure 4C). Notch 1 and 2 were expressed on CMPs, megakaryocyte and erythroid progenitors (MEPs), and granulocyte-macrophage progenitors (GMPs) (Akashi et al., 2000). Of note, Notch1 showed the lowest expression in MEP, whereas Notch4 showed the highest expression in MEP and was not detectable in GMP. Notch3 expression was not detected in any cell population (data not shown). The Notch targets Hes1 and Hey1 showed the highest expression in MEP, intermediate expression in CMP, and minimal expression in GMP, and Hes5 was only expressed in CMP and MEP (Figure 4D). The correlation between expression of Notch receptors and their transcriptional targets indicated that the Notch signaling pathway had been activated in CMP and MEP in vivo. In order to assess the biological effect of Notch pathway stimulation on these progenitors, CMP, MEP, and GMP were flow sorted and plated on stroma. Both CMP and MEP plated on OP9-DL1 differentiated preferentially toward the megakaryocyte lineage compared to those plated on OP9-GFP cocultures (Figures 4E and 4F) and showed an increased CFU-Mk potential after replating in methylcellulose or collagen-based semisolid cultures (Figure S3). GMP plated on OP9-DL1 showed a reduced differentiation toward Mac1^{hi} myeloid cells compared to OP9-GFP cocultures and did not show any megakaryocyte development (Figure S5A). Of note, GMP plated on OP9-DL1 for 24 hr showed an increase in apoptosis compared to OP9-GFP cocultures,

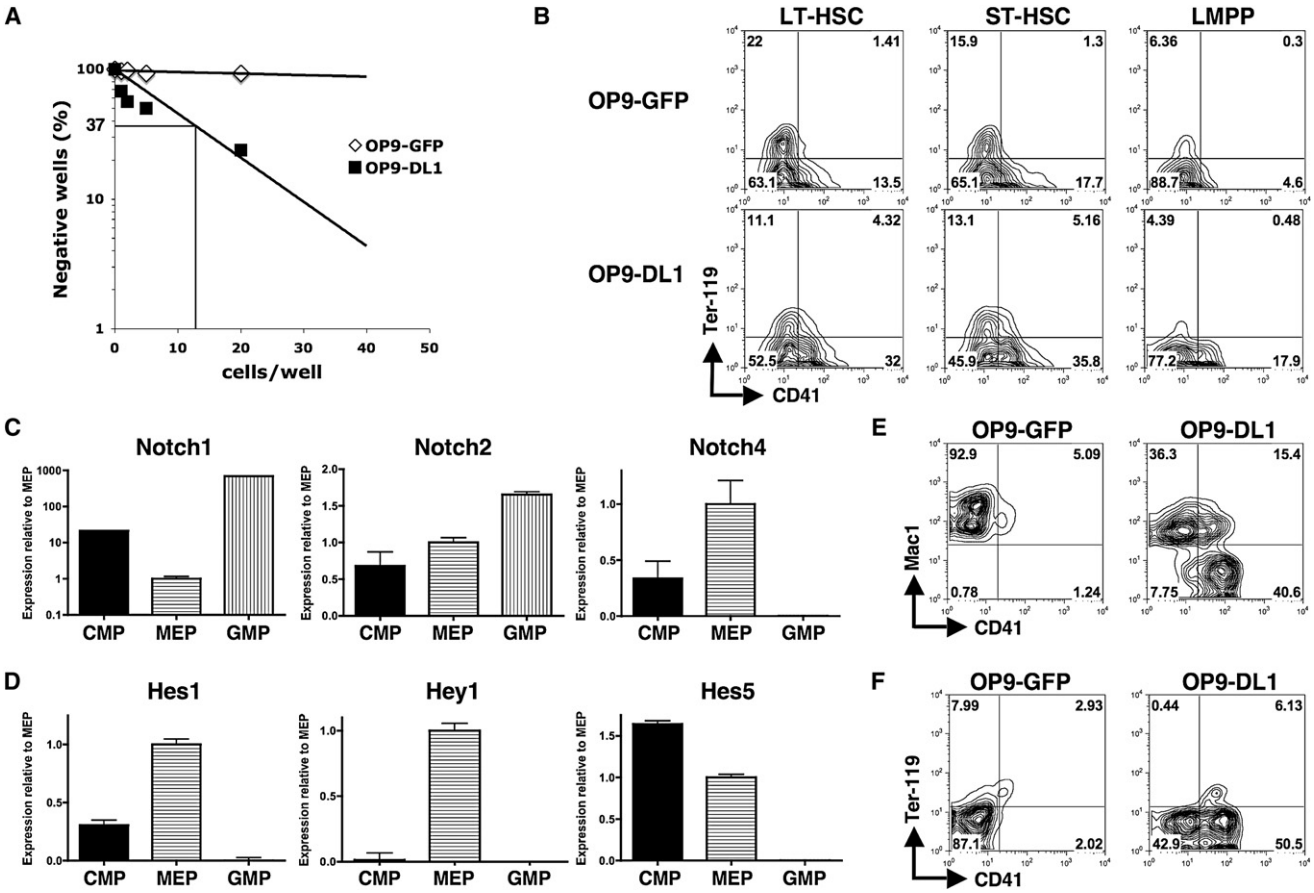

Figure 4. Notch Specifies Megakaryocyte Fate at Several Levels of Hematopoietic Differentiation

(A) Limiting dilution assay with LSK cells from wild-type murine bone marrow directly sorted into individual OP9-GFP or OP9-DL1-coated 96-well plates with 1, 2, 5, or 20 cells per well and cultured for 8 days. Cocultures were analyzed under a microscope: wells with visible hematopoietic cells were scored and megakaryocytes were counted. Frequency of megakaryocyte-containing wells is represented, and trend lines were used to estimate the frequency of megakaryocyte-forming cells in the LSK population.

(B) Flow-sorted Lin$^-$Sca1$^+$Kit$^+$CD34$^-$Flt3$^-$ (LT-HSC), Lin$^-$Sca1$^+$Kit$^+$CD34$^+$Flt3$^-$ (ST-HSC), and Lin$^-$Sca1$^+$Kit$^+$CD34$^+$Flt3$^+$ (LMPP) cells were plated directly onto OP9-GFP or OP9-DL1 stroma. Flow cytometric analysis was performed after 7 days of coculture.

(C and D) RNA from flow-sorted CMP, MEP, and GMP were extracted, amplified, and used for analysis of quantitative expression of Notch receptors (C) and the Notch targets Hes-1, Hes-5, and Hey-1 (D). Results were normalized to GAPDH expression and to the MEP value. Notch3 expression was not detected in any sample. Error bars represent SEM.

(E) Flow-sorted CMP were cultured on OP9-GFP or OP9-DL1 for 5 days before analysis by flow cytometry.

(F) Flow-sorted MEP were cultured on OP9-GFP or OP9-DL1 for 3 days before analysis by flow cytometry.

whereas no significant difference in apoptosis was observed with MEP (Figure S5B). At the level of MEP, DL1 stimulation resulted in increased expression of several Notch targets including Hes1, Hey1, and Nrarp as well as genes important for megakaryopoiesis including Gata1, Gata2, and Fli1 (Figure S4C). Of interest, the Notch-induced megakaryocyte differentiation of CMP and MEP was potentiated by addition of low concentrations of TPO in OP9-DL1 cocultures (Figure S6). In addition, the TPO-induced megakaryocyte differentiation observed on OP9-GFP was significantly inhibited by γ-secretase inhibitor treatment (Figure S6), suggesting a potential crosstalk between the Notch and TPO/MPL signaling pathways during megakaryocyte differentiation. Together, these results suggest that the Notch signaling pathway is activated in myeloid-committed CMP and MEP in vivo and favors megakaryocytic fate through concomitant induction of a megakaryocytic transcriptional program and apoptosis in the GMP compartment.

Inhibition of Notch Signaling Impairs Megakaryopoiesis In Vivo

We next assessed the effects of Notch signaling on megakaryocyte development in vivo using bone marrow transplantation assays with wild-type bone marrow cells transduced with murine ecotropic retrovirus encoding dnMAML1 or empty vector controls (MIG). Expression of dnMAML1 resulted in a reduction in the number of MEP and megakaryocyte progenitors (c-Kit$^+$CD41$^+$) (Figures 5A and 5B, respectively). In addition, dnMAML1-expressing cells showed a significant reduction in the number of maturing megakaryocyte as assessed by the presence of CD41$^+$, CD42b$^+$, or CD41/CD61$^+$ cells in the bone

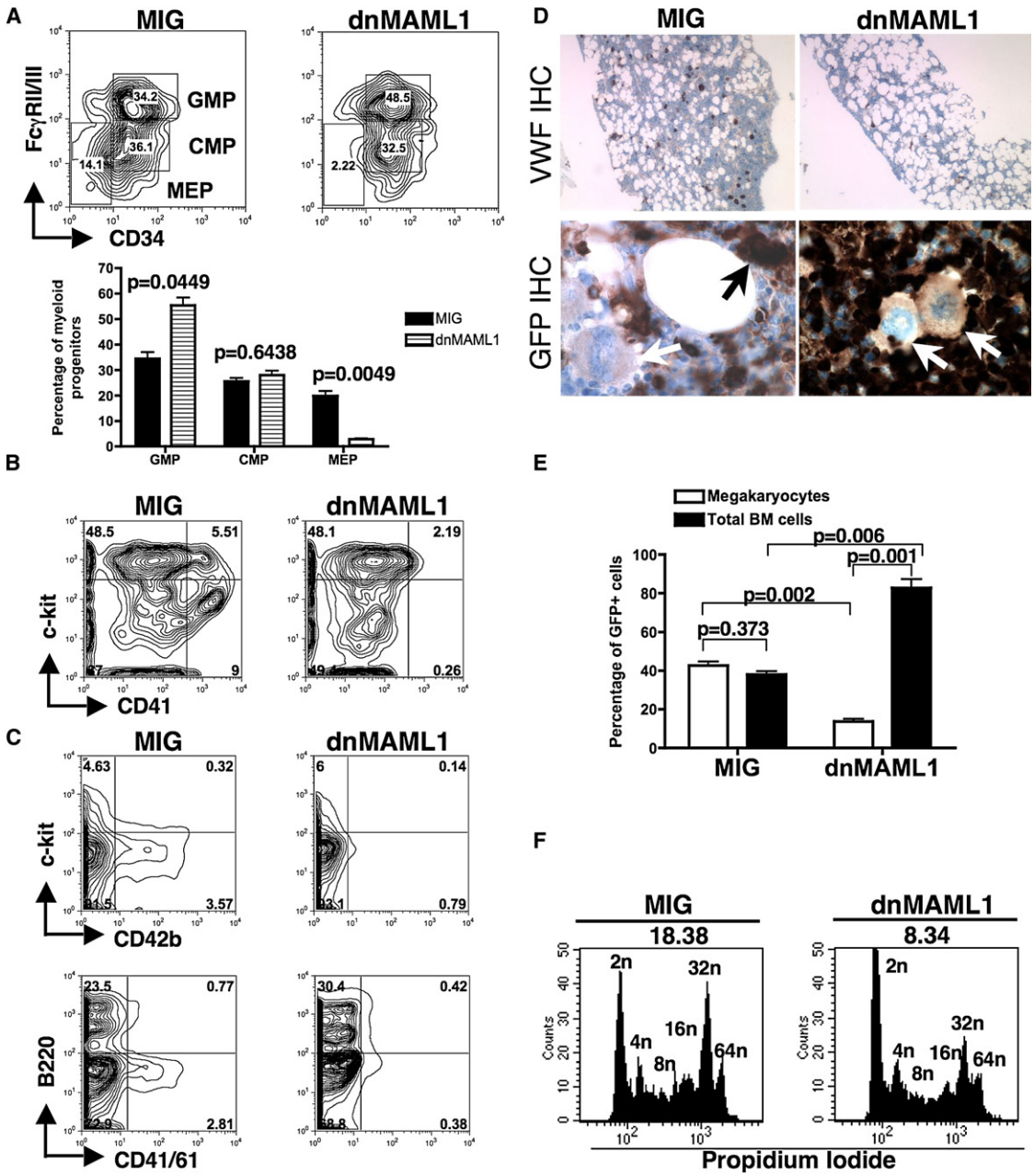

Figure 5. DnMAML1 Inhibits Megakaryocyte Development In Vivo

(A) Wild-type bone marrow cells were infected with dnMAML1-encoding or MIG control retroviruses and injected into lethally irradiated syngeneic recipients. Analysis was performed after 3–6 weeks. Flow cytometric analysis of myeloid progenitors within the Lineage$^-$cKit$^+$Sca1$^-$ population. Analysis was gated on GFP$^+$ cells. A representative of five independent animals is shown for each group. Mean ± SEM for a total of five independent animals is represented below as histograms.

(B) Analysis of the megakaryocyte progenitors c-Kit$^+$CD41$^+$ population (gated on Lineage$^-$ GFP$^+$cells) in the bone marrow of MIG versus dnMAML1 recipient animals.

(C) FACS analyses of GFP$^+$ dnMAML1 recipient bone marrow cells indicate impaired megakaryocyte development compared to MIG control recipients.

(D) Immunohistochemical (IHC) analysis of consecutives bone marrow sections shows reduced staining for the megakaryocyte-specific vWF and mostly GFP$^-$ megakaryocytes in dnMAML1 recipients, compared to MIG controls. For both vWF and GFP immunostainings, positive cells show a dark brown color. Black and white arrowheads indicate GFP$^+$ and GFP$^-$ megakaryocytes, respectively. Original magnifications are ×100 (vWF) and ×1000 (GFP).

(E) Fifty megakaryocytes were counted on bone marrow sections stained for GFP, and the percentages of GFP+ megakaryocytes are shown (white histograms). The percentages of GFP$^+$ total bone marrow (BM) cells were assessed in the same recipients by flow cytometry and are also shown (black histograms). Histograms represent mean ± SEM of three independent animals for each group.

(F) Ploidy analysis was performed by flow cytometry using propidium iodide and gating on GFP$^+$CD41$^+$ megakaryocytes. Median ploidy is indicated above the histogram (value for diploid state = 2).

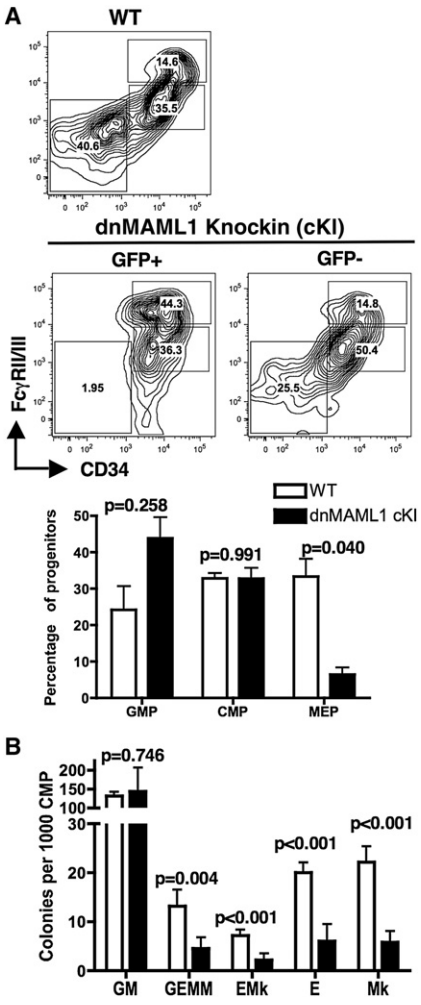

Figure 6. DnMAML1 Conditional Knockin Mice Have Impaired Megakaryopoiesis

(A) DnMAML1 cKI-Mx1Cre double transgenic animals were induced with poly(I:C) at 6 weeks of age and analyzed 2–3 weeks later. A representative flow cytometric analysis of myeloid progenitors within the Lineage$^-$cKit$^+$Sca1$^-$ population is shown. Mean ± SEM of three independent analyses gated on GFP$^+$ cells is shown below as histograms.

(B) Flow-sorted CMPs were plated in methylcellulose cultures supplemented with IL3, IL6, SCF, EPO, and TPO, and colonies were counted after 7 days. GM, granulocyte-macrophage colony; GEMM, granulocyte-macrophage-erythroid-megakaryocyte colony; EMk, erythroid-megakaryocyte colony; E, erythroid colony; Mk, megakaryocyte colony; cKI, conditional knockin. Mean ± SEM (n = 3) are shown.

marrow (Figure 5C and Figure S7A). This finding was supported by histological analyses of bone marrow sections of these recipients showing decreased numbers of mature von Willebrand Factor (vWF)$^+$ megakaryocytes in dnMAML1 recipients. Of note, although GFP expression in total bone marrow cells was high in dnMAML1 recipients (82% ± 13%), those mature megakaryocytes that were present in animals transduced with dnMAML1 displayed low to absent GFP expression by immunohistochemistry (Figures 5D and 5E). This observation suggests that megakaryocyte development only occurred in untransduced cells or in cells that expressed very low levels of dnMAML1. Bone marrow cellularity and platelet counts were comparable between dnMAML1 and MIG control transplanted animals (Figure S8 and data not shown). DNA content analysis of bone marrow-derived megakaryocytes showed a reduced median ploidy of GFP$^+$CD41$^+$ megakaryocytes in dnMAML1 recipients compared to control animals (Figure 5F).

To exclude the possibility that dnMAML1-expressing hematopoietic progenitors fail to engraft properly, we analyzed a transgenic mouse harboring a dnMAML1-GFP fusion conditional knockin allele (dnMAML1 cKI) (Maillard et al., 2008; Tu et al., 2005). In this model, dnMAML1 expression is induced in adult dnMAML1 cKI-Mx1Cre double transgenic mice by injection of poly(I:C). Compared to LSK cells derived from Mx1Cre-only control animals, LSK cells derived from conditional dnMAML1 cKI-Mx1Cre animals 2 to 3 weeks after pIpC injection did not differentiate efficiently toward megakaryocytes when plated on OP9-DL1 stroma (Figure S7B), similar to LSK cells transduced with the dnMAML1-encoding retrovirus. In addition, dnMAML1-induced animals showed a significant reduction in the numbers of MEP, but not CMP or GMP compared to controls, specifically in dnMAML1-expressing GFP$^+$ cells (Figure 6A). As the MEP population was barely detectable in dnMAML1 cKI animals, functional validation of the megakaryocyte potential in dnMAML1-expressing progenitors was obtained by assessing myeloid-colony-forming potential of the CMP population. GFP$^+$ CMP from dnMAML1 animals displayed a significantly decreased potential to form either megakaryocyte- or erythrocyte-containing colonies, but not granulocyte-macrophage colonies, compared to control CMP (Figure 6B). Of further interest, dnMAML1-expressing CMP showed reduced expression levels of several Notch targets such as Hes1, Hes5, and Hey1 (Figure S7C). These data together indicate that the development of MEPs and megakaryocyte progenitors, as well as subsequent megakaryocyte maturation, is impaired in vivo by dnMAML1, a global inhibitor of canonical Notch signaling.

ICN4 Expression Supports Megakaryopoiesis In Vivo

We next performed bone marrow transplants with cells transduced with ICN4 to assess the effect of increased Notch signaling on megakaryopoiesis in vivo. To preclude confounding results related to development of T cell leukemia in this model system, we used Rag1$^{-/-}$ bone marrow as a source of donor cells (Pear et al., 1996; Stier et al., 2002). Flow cytometric analysis showed a significant increase in the number of MEP in ICN4-expressing GFP$^+$ cells compared to MIG controls (Figures 7A and 7B). In contrast, the number of GMPs, as well as c-Kit$^+$CD71$^+$ and c-Kit$^-$CD71$^+$ erythroid progenitors, was reduced in ICN4 recipients compared to control animals (Figure 7A and Figure S9). Accordingly, bone marrow cells from ICN4 animals gave rise to a higher number of CFU-MK colonies compared to control recipients (Figure 7C). In addition, immunohistochemistry of bone marrow sections for GFP and vWF showed an increase in the absolute number of mature megakaryocytes in ICN4 animals (Figure 7D). Most megakaryocytes were GFP$^+$, although GFP expression in total bone marrow cells was low (Figure 7E), indicating selectivity for megakaryocyte fate among cells expressing ICN4. Of note, bone marrow cellularity and platelet counts in ICN4 animals were similar to

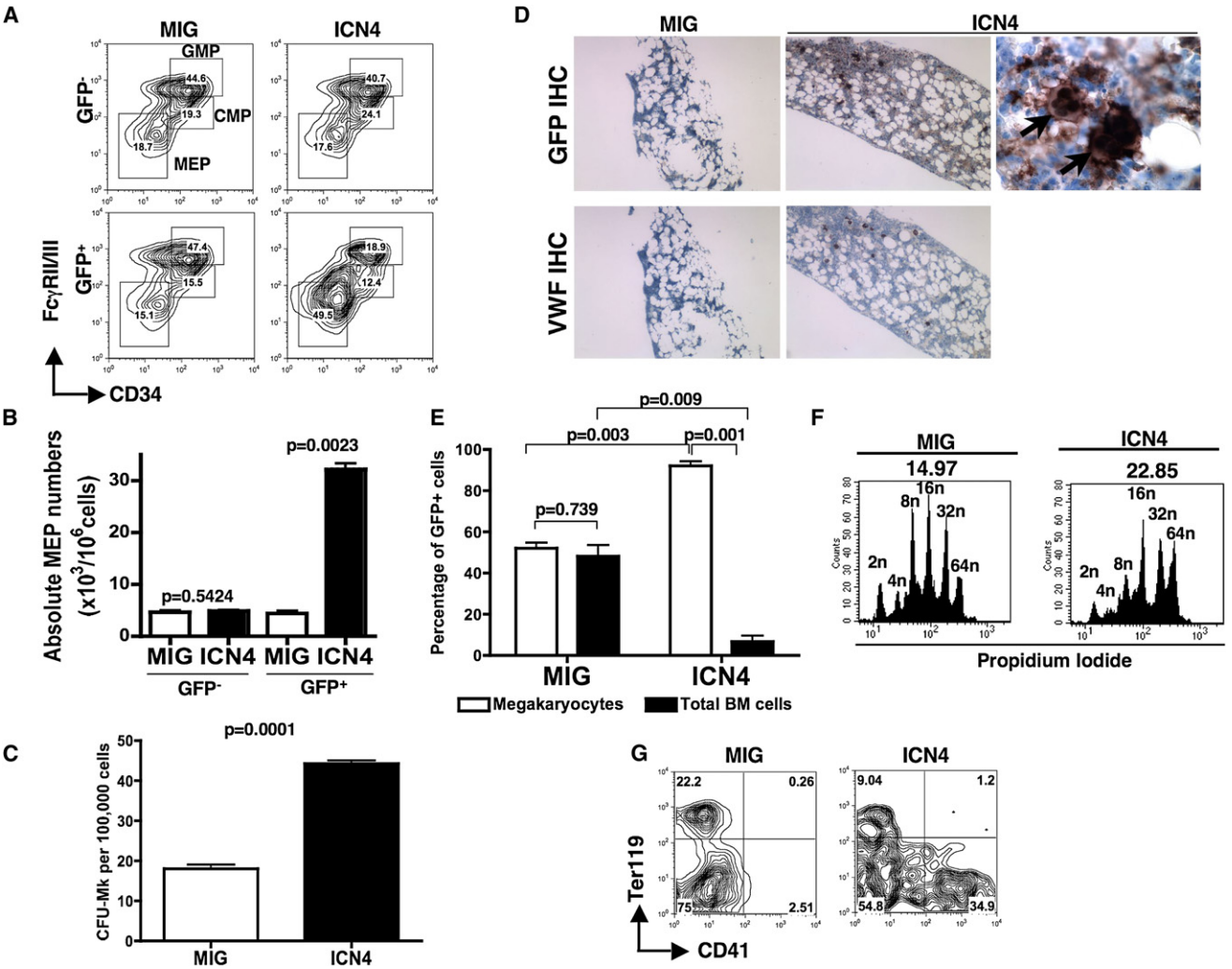

Figure 7. ICN4 Supports Megakaryocyte Development In Vivo

(A) Rag1$^{-/-}$ bone marrow cells were infected with ICN4-encoding or MIG control retroviruses and injected into wild-type lethally irradiated C57BL/6 recipients. The MEP population was analyzed by flow cytometry. Representative analysis of myeloid progenitor populations in ICN4 recipients compared to controls (GFP$^+$ or GFP$^-$ gated population is indicated on the left side).

(B) Absolute numbers of MEP are indicated as mean ± SEM of three independent analyses.

(C) Megakaryocyte colony-forming unit (CFU-MK) potential from total bone marrow. Mean ± SEM of quadruplicate experiments is represented.

(D) Consecutive bone marrow sections from ICN4 and MIG recipients were stained as in Figure 5D. Arrowheads indicate GFP$^+$ megakaryocytes. Original magnification in the upper left four panels is ×100 and in the upper right panel is ×1000.

(E) The number of GFP$^+$ megakaryocytes and bone marrow (BM) cells were assessed as in Figure 5E. Histograms represent mean ± SEM of three independent animals in each group.

(F) Flow cytometric analysis of megakaryocyte ploidy gated on GFP$^+$CD41$^+$ cells. Median ploidy is indicated in the histograms (value for diploid state = 2).

(G) Flow-sorted MEPs from the bone marrow of wild-type C57BL/6 animals were retrovirally transduced with empty control (MIG), ICN1, or ICN4 retroviruses and injected into lethally irradiated recipients with 2 × 10^5 helper bone marrow cells. Bone marrow cells from recipients were analyzed 12 days posttransplant and analysis was gated on GFP$^+$ cells.

MIG control animals (Figure S8 and data not shown). Furthermore, ploidy analysis revealed increased median ploidy content of ICN4-expressing megakaryocytes (Figure 7F). Finally, to confirm the role of Notch signaling on MEP in a Rag wild-type context, we performed bone marrow transplantation with flow-sorted MEPs from wild-type animals transduced with ICN4. Analysis 12 days after transplant showed that ICN4 expression in MEP resulted in increased megakaryocyte differentiation and reduced erythroid differentiation in vivo (Figure 7G). Taken together, these data indicate that Notch4 signaling favors MEP at the expense of GMP development and subsequently potentiates megakaryopoiesis in vivo.

DISCUSSION

In toto, the present study shows that Notch signaling influences megakaryocytic fate at several stages of primary hematopoietic stem and progenitor cell differentiation both in vitro and in vivo

(Figure S10). First, these findings support a role for Notch signaling in the development of common MEPs from LSK cells and the concomitant inhibition of GMPs. The latter observation is in accord with previous reports showing an inhibitory effect of Notch signaling on granulocyte-macrophage differentiation (de Pooter et al., 2006; Stier et al., 2002). Our results suggest that Notch-induced megakaryocyte specification is mediated by both induction of a megakaryocytic transcriptional program and selective induction of apoptosis in the GMP compartment, reminiscent of the role of Notch during T versus B lymphocyte differentiation. Of interest, Notch-induced megakaryopoiesis was significantly more efficient from LT- and ST-HSCs than from LMPPs, suggesting that although canonical Notch signaling is dispensable for HSC maintenance (Maillard et al., 2008), it plays a role in their differentiation. As reported recently, the $Flt3^+MPL^+LSK$ population, a subfraction of the LMPP compartment, may be responsible for the residual erythromegakaryocytic potential of the LMPP (Luc et al., 2008). Together, these results support an early commitment to the erythromegakaryocytic lineage that branches from LT/ST-HSC prior to lymphoid commitment (Adolfsson et al., 2005; Forsberg et al., 2006; Luc et al., 2008; Pronk et al., 2007). In addition, these data suggest that Notch signaling subsequently plays an important role in the differentiation of megakaryocytic versus erythrocytic cells. Indeed, although we observed an increase in the CFU-E potential after short exposure of LSK cells to Notch ligand in vitro, consistent with previous observations (Dando et al., 2005) and with an increased differentiation toward MEP, further development of the erythroid lineage was inhibited by Notch pathway activation in vitro and in vivo, as previously shown in vitro in the context of the erythromegakaryocytic K562 cell line (Ishiko et al., 2005; Lam et al., 2000).

Global expression profiling of LSK cells grown on OP9-DL1 stromal cells using GSEA analysis suggests coordinate regulation of Notch signaling with engagement of transcriptional programs that favor megakaryocytic development. Hes factors are upregulated by DL1 stimulation and recapitulate, at least partially, the effect of Notch pathway stimulation on megakaryocyte development when expressed in LSK cells. Nevertheless, it is likely that other direct or indirect targets of the Notch signaling pathway are required to achieve maximal megakaryocyte development. Of note, we observed an increased expression of the transcription factors *GATA-1*, *GATA-2*, and *FOG1/ZFPM1* that are required for normal megakaryocyte development (Chang et al., 2002; Shivdasani et al., 1997; Tsang et al., 1997) following Notch stimulation of LSK cells. These observations are in consonance with reports of Notch signaling promoting transcription of the GATA factor Serpent (Mandal et al., 2004) in *Drosophila* and expression of GATA-3 factor during T cell development in mammals (Amsen et al., 2007; Fang et al., 2007) through an $RBPJ\kappa$-dependent mechanism. Other reports indicate that Notch directly controls GATA-2 expression in early hematopoietic progenitors (de Pooter et al., 2006; Kumano et al., 2001). By analogy, Notch signaling may play a similar role in megakaryocyte development by regulating expression and function of GATA-1, GATA-2, or FOG1. In addition, our findings indicate that Notch stimulation also results in upregulation of cytokine receptors as well as structural proteins important for megakaryocyte development. Of further interest, Notch has been reported to induce transition from mitotic cell cycle to endocycle in *Drosophila* follicle cells (Deng et al., 2001), suggesting that Notch might also be involved in initiation of polyploidization, a hallmark of megakaryocyte differentiation. Together, these data suggest that Notch signaling may be a master regulator of several genes critical for early megakaryocyte commitment from hematopoietic stem and progenitor cells.

The mammalian Notch signaling pathway is complex, cell context dependent, and involves multiple ligands and receptors (Bray, 2006; Nam et al., 2007). Genetic pleiotropy among the Notch ligands and receptors in mammals may be necessary for regulation of cell-fate decisions at multiple branch points in hematopoietic development (Radtke et al., 2004a). Our findings are consistent with a positive role of DL1, Notch1, and Notch4 during megakaryocyte fate determination. Of note, ICN4 expression in LSK cells resulted primarily in the development of $CD41^+$ cells, whereas ICN1 also promoted significant development of $Ter119^+CD41^+$ cells in vitro. In addition, Notch1 showed the lowest expression in MEP, whereas Notch4 showed the highest expression in this progenitor population, suggesting a physiological role for Notch4 in megakaryocyte differentiation. Finally, only ICN4 expression in MEP resulted in increased megakaryocyte differentiation in vivo. These results suggest a potential stage-specific role for Notch receptors during erythromegakaryocyte and subsequent erythroid or megakaryocyte lineage commitment. A role for Jagged ligands in megakaryopoiesis in vivo seems less likely, given that culture of LSK cells on parental OP9 stroma, known to express both Jagged1 and Jagged2 (Schmitt and Zuniga-Pflucker, 2002), does not result in significant megakaryocyte development. However, further studies are needed to characterize the Notch receptors, ligands, and cellular targets that regulate megakaryocyte development in vivo. Of interest, our data indicate that Notch stimulation potentiates TPO-induced megakaryopoiesis of several hematopoietic progenitors in vitro. Therefore, assessment of the interactions and potential cooperative effects with cytokines signaling (i.e., the TPO/MPL axis) during megakaryopoiesis will also be important.

Finally, these findings may have important clinical and therapeutic implications. For instance, they suggest the possibility that Notch pathway blockade may be of potential value in hematological malignancies associated with megakaryocytic hyperplasia, including essential thrombocythemia, polycythemia vera, myeloid metaplasia with myelofibrosis, or acute megakaryoblastic leukemia (AMKL). The importance of Notch signaling in the latter is supported by our recent findings that the OTT-MAL (also known as RBM15-MKL1) fusion protein, exclusively associated with this type of AMKL, interacts with RBPJ through its OTT moiety and alters its transcriptional properties (T.M., M.G.C., and D.G.G., unpublished data). In addition, our results suggest that Notch pathway stimulation may be of value in enhancing megakaryocyte growth and platelet production in clinical contexts associated with severe thrombocytopenia, such as hematopoietic reconstitution following bone marrow transplantation or chemotherapy.

EXPERIMENTAL PROCEDURES

Coculture of Sorted Progenitors and Stromal Cells

OP9-GFP and OP9-DL1 stromal cells (a kind gift of Dr. Carlos Zúñiga-Pflücker) were cultured in "OP9-media": α-MEM (StemCell Technologies) containing

20% FCS (GIBCO), 50 μM 2-mercapto-ethanol (Chemicon), 2 mM glutamine (GIBCO), 0.2% sodium bicarbonate (GIBCO), 100 U/ml penicillin, and 0.1 mg/ml streptomycin (GIBCO). The OP9 cells were plated on day 0 in 24-well plates at a density of 2×10^4 cells/well. On day 1, 5×10^2–2×10^4 sorted progenitors were plated onto the stroma in OP9 media, and half of the media was changed every 3 days. γ-secretase activity was inhibited with Compound E (γ-secretase inhibitor XXI, Calbiochem) or DAPT (γ-secretase inhibitor IX, Calbiochem) at a final concentration of 1 μM. DMSO was used as vehicle-only control. TPO (Peprotech) was used at the indicated concentrations. For analysis, hematopoietic cells were harvested from the supernatant of the cultures and filtered through a 100 μm strainer. For microarray analysis, cells harvested from the coculture were incubated for 1 hr in OP9 media on tissue-culture treated plates, and only supernatants were collected to remove any residual stromal cells before RNA extraction.

Flow Cytometric Analysis and Cell Sorting

All antibodies were obtained from BD PharMingen except anti-CD42b and anti-CD41/CD61 (clone Xia.G5 and clone Leo.D2, respectively, Emfret), and staining procedures were performed in PBS/2% FBS. For purification of LSK by flow cytometry, murine bone marrow cells were first magnetically depleted of lineage-positive cells with a cocktail of rat anti-mouse antibodies against all mature blood cells, including Ter119, B220, CD3, CD4, CD8, IL7-R, CD19, and Gr1. Residual lineage-positive cells were detected using a goat-anti-rat PE-Cy5.5-conjugated antibody. To obtain LSK cells, cells were subsequently stained with anti-CD34, c-kit, Sca-1 (BD PharMingen), and Fcγ-RII/III (Abcam) antibodies and sorted using a FACSAria (BD Biosciences). Human CD34+ bone marrow cells were obtained from AllCells. For in vitro cocultures of LSK cells with stroma, analyses were gated on forward/side scatter profile and $CD45^+$ or $CD45^+GFP^+$ cells. Apoptosis assays were performed following the manufacturer's recommendations (AnnexinV-FITC Apoptosis Detection Kit I, BD PharMingen). For ploidy analysis of LSK cells cocultured on OP9-GFP or OP9-DL1 stroma at day 8, cells in the supernatant were stained with anti-CD41-FITC and anti-CD45-APC antibodies. For ploidy analysis of bone marrow transplant recipients, bone marrow cells were cultured in RPMI1640 + 10% FBS + 10 ng/ml of TPO for 4 days prior to fixation with 1% PFA and staining with a primary rat anti-mouse CD41 and a secondary APC-conjugated anti-rat antibody. In both cases, cells were subsequently incubated with 0.1% sodium citrate solution containing 50 μg/ml RNase and 50 μg/ml propidium iodide. Analysis was gated on $CD41^+CD45^+$ and $CD41^+GFP^+$ cells, respectively. Data were analyzed using FlowJo or CellQuest (BD Biosciences) software.

Staining and Immunohistochemistry

Cytospins of hematopoietic cells from cocultures were prepared on glass slides (Cytospin4, ThermoShandon). Slides were stained using Wright-Giemsa Solutions (Sigma Diagnostics) or AchE staining solution (Stem Cell Technologies) following manufacturer's recommendation. vWF (Dakocytomation) and green fluorescent protein (GFP, Clone JL-8; Clontech, Palo Alto, CA) antibodies were used to perform immunohistochemistry on paraffin-embedded tissue sections at the Dana Farber/Harvard Cancer Center Specialized Histopathology Services Core facility. CFU-MK potential was assessed using MegaCult-C following the manufacturer's recommendations (StemCell Technologies). Images were obtained using a Nikon Eclipse E400 microscope with a 10×/22 NA ocular lens (Nikon, Tokyo, Japan) and a SPOT RT color digital camera (model 2.1.1; Diagnostic Instruments). Low-power images (magnification ×100) were obtained with a 10×/0.25 objective lens, intermediate power images (magnification ×400 and ×600) with a 40×/1.3 NA and 60×/1.4 objective lenses with oil, and high-power images (×1000) with a 100×/1.4 objective lens with oil (Trak 300; Richard Allan Scientific). Images were analyzed using Adobe Photoshop 6.0 (Adobe Systems).

RNA Extraction, Real-Time RT-PCR, and Microarray Analyses

RNA from LSK cells cocultured with OP9-GFP or OP9-DL1 cells for 5 days was isolated using the RNeasy Mini Kit (QIAGEN). Expression levels of Gata-1 (Mm00484678_m1 assay, Applied Biosystems), PU.1/SFPI-1 (Mm00488140_m1 assay, Applied Biosystems), Hes-1 (Mm00468601_m1 assay, Applied Biosystems), Hes-5 (Mm00439311_g1, Applied Biosystems), Hey-1 (Mm00468865_m1, Applied Biosystems), Nrarp (Mm00482529_s1, Applied Biosystems), Fli-1 (Mm00484410_m1 assay, Applied Biosystems), Notch1 (Mm00435245_m1, Applied Biosystems), Notch2 (Mm00803077_m1, Applied Biosystems), Notch3 (Mm00435270_m1, Applied Biosystems), and Notch4 (Mm00440525_m1, Applied Biosystems) were assessed by quantitative RT-PCR (EZ RT-PCR Core Reagents, Applied Biosystems) following the manufacturer's recommendations and normalized to GAPDH (assay number 4352932E, Applied Biosystems).

For microarray analysis, RNA from LSK cells cultured 3 days on OP9-GFP, OP9-DL1, or OP9-DL1 supplemented with Compound E was extracted using the RNEasy Micro Kit (QIAGEN) following the manufacturer's recommendations. For each condition, 25 ng of RNA was amplified and biotin labeled using the Ovation Biotin system (Nugen) following the manufacturer's recommendations. The labeled probes were then hybridized to Affymetrix (San Jose, CA) Mouse Genome 430.2 (MOE430_2) GeneChip Arrays (45101 probe sets). The ".CEL" files from the MAS5 software were used as starting points for all analyses (three replicates per condition). Data were analyzed by using the R statistical package bioconductor and data quality assessed by using functions in the Affy and AffyPLM packages. The GCRMA algorithm (2.4.1) was used to obtain normalized expression estimates. Genes that were selected for further analysis had probe sets for which the expression value was greater than 27(log2) (which in our study constitutes the average background reading for all probe sets) and a present flag call in at least two of three samples. To detect significant changes in the expression levels, two-sample Welch t tests (parametric; assuming unequal variances; Benjamini and Hochberg step-up multiple testing correction at a false discovery rate < 0.05) were applied to the resulting genes. The resulting mouse genes associated with Mouse Genome 430 2.0 GeneChip arrays were extracted via the NetAffx Gene Ontology Mining tool (Affymetrix). The "Notch Gene List" and the "Megakaryocyte Gene List" were generated based on the available literature reporting these genes as involved in the Notch signaling pathway or upregulated during megakaryocyte differentiation, respectively. These gene lists were subsequently used in all GSEAs (Subramanian et al., 2005). The leading edge subset of genes was determined by the GSEA criteria "core enrichment." The data discussed in this publication have been deposited in NCBI's Gene Expression Omnibus and are accessible through GEO Series accession number GSE11723.

Viral Infection, Bone Marrow Transplantation, and Poly(I:C) Injection

MSCV-DN-MAML1-GFP (kind gift from Dr. James D. Griffin), MSCV-IRES-GFP (MIG)-ICN1, MIG-Hes1, MIG-Hes5 (kind gifts from Dr. Catherine Lavau) (Kawamata et al., 2002), and MIG-ICN4 constructs are described elsewhere. Viral supernatants were obtained as described previously (Mercher et al., 2006). Similar viral titers were used for each retroviral construct, and transduction efficiencies in primary cells were confirmed for the various constructs by flow cytometric analysis of GFP content. For transduction, 2×10^4 sorted LSK cells were directly spin infected for 60 min at 2000 rpm with viral supernatant in IMDM containing 20% FBS, 20 ng/mL mIL6 (R&D systems), 10 ng/mL mSCF (Peprotech, Rocky Hill, NJ), 10 ng/mL mIL11 (Peprotech, Rocky Hill, NJ), 5 μg/mL Polybrene (American Bioanalytical), and 7.5 mM HEPES buffer (GIBCO). Cells were incubated overnight in the same media and washed and plated in OP9 media on stroma for 5–10 days before flow cytometric analysis. For bone marrow transplantation, $Rag1^{-/-}$ (Jackson Laboratories) or wild-type (Taconic) 8- to 10-week-old C57BL/6 donor mice were injected with 5-FU (Sigma) 5 days prior to bone marrow collection from femurs and tibiae. After an overnight incubation in RPMI1640 supplemented with 10% FBS, 10 ng/mL mIL-3, 20 ng/mL mIL-6, and 10 ng/mL mSCF, cells were spin infected with viral supernatants two times on day 1 and 2, and 1×10^6 were injected into the tail vein of lethally irradiated wild-type C57BL/6 recipient mice. Animals were analyzed 5–8 weeks after transplantation. For transplantation with MEP, MEP were flow sorted and directly infected once with MIG, ICN1, or ICN4 retroviruses, and 5×10^4 MEPs were injected into the tail vein of lethally irradiated wild-type C57BL/6 recipients along with 2×10^5 helper whole bone marrow cells. Animals were analyzed 12 days after injection. DnMAML1-GFP conditional knockin mice (Tu et al., 2005) were crossed with Mx1-Cre (Jackson Laboratories). Double transgenic animals were induced at 6 weeks of age with six to eight intraperitoneal injections of poly(I:C) (Sigma, 500 μg per injection) and analyzed 2–3 weeks later. Poly(I:C) injections lead to excision of the Stop cassette in front of the dnMAML1-GFP allele and expression of the dnMAML1-GFP fusion, which can be tracked by flow cytometry for GFP. Mx1-Cre transgenic animals injected with poly(I:C) were used as

wild-type controls. Approval for the use of animals in this study was granted by the Children's Hospital Boston Institutional Animal Care and Use Committee (IACUC).

Statistical Analysis

Statistical significance of differences between the different conditions was assessed using a two-tailed unpaired t test.

SUPPLEMENTAL DATA

The Supplemental Data include ten figures and two tables and can be found with this article online at http://www.cellstemcell.com/cgi/content/full/3/3/314/DC1/.

ACKNOWLEDGMENTS

We are very grateful to Dr. J.C. Zúñiga-Pflücker for the OP9-GFP and OP9-DL1 cells; Dr. C. Lavau for the ICN1, Hes1, and Hes5 constructs; and Dr. J.D. Griffin and Dr. Lizi Wu for the dnMAML1 construct. We are very grateful to Dr. O. Shestova and Dr. M. Santos for help with dnMAML1 transgenics. We thank A. Fabian for technical assistance with cell sorting and Dr. J.L. Kutok and the Dana Farber Histopathology Core Facility for histology studies. T.M. is a recipient of a Leukemia and Lymphoma Society Special Fellow Award. D.G.G. is a Doris Duke Foundation Distinguished Clinical Scientist and a Howard Hughes Medical Institute investigator. This work was supported in part by National Institute of Health grants AI047833 (W.S.P.), CA119070 (J.C.A.), and DK50654 and CA66996 (D.G.G.) and by the Leukemia and Lymphoma Society to W.S.P., J.C.A., and D.G.G. The authors declare no competing financial interests.

Received: March 12, 2008
Revised: June 14, 2008
Accepted: July 16, 2008
Published: September 10, 2008

REFERENCES

Adolfsson, J., Mansson, R., Buza-Vidas, N., Hultquist, A., Liuba, K., Jensen, C.T., Bryder, D., Yang, L., Borge, O.J., Thoren, L.A., et al. (2005). Identification of Flt3+ lympho-myeloid stem cells lacking erythro-megakaryocytic potential a revised road map for adult blood lineage commitment. Cell *121*, 295–306.

Akashi, K., Traver, D., Miyamoto, T., and Weissman, I.L. (2000). A clonogenic common myeloid progenitor that gives rise to all myeloid lineages. Nature *404*, 193–197.

Amsen, D., Antov, A., Jankovic, D., Sher, A., Radtke, F., Souabni, A., Busslinger, M., McCright, B., Gridley, T., and Flavell, R.A. (2007). Direct regulation of gata3 expression determines the T helper differentiation potential of notch. Immunity *27*, 89–99.

Besseyrias, V., Fiorini, E., Strobl, L.J., Zimber-Strobl, U., Dumortier, A., Koch, U., Arcangeli, M.L., Ezine, S., Macdonald, H.R., and Radtke, F. (2007). Hierarchy of Notch-Delta interactions promoting T cell lineage commitment and maturation. J. Exp. Med. *204*, 331–343.

Bray, S.J. (2006). Notch signalling: a simple pathway becomes complex. Nat. Rev. Mol. Cell Biol. *7*, 678–689.

Chang, A.N., Cantor, A.B., Fujiwara, Y., Lodish, M.B., Droho, S., Crispino, J.D., and Orkin, S.H. (2002). GATA-factor dependence of the multitype zinc-finger protein FOG-1 for its essential role in megakaryopoiesis. Proc. Natl. Acad. Sci. USA *99*, 9237–9242.

Dando, J.S., Tavian, M., Catelain, C., Poirault, S., Bennaceur-Griscelli, A., Sainteny, F., Vainchenker, W., Peault, B., and Lauret, E. (2005). Notch/Delta4 interaction in human embryonic liver CD34+ CD38− cells: positive influence on BFU-E production and LTC-IC potential maintenance. Stem Cells *23*, 550–560.

de Pooter, R.F., Schmitt, T.M., de la Pompa, J.L., Fujiwara, Y., Orkin, S.H., and Zuniga-Pflucker, J.C. (2006). Notch signaling requires GATA-2 to inhibit myelopoiesis from embryonic stem cells and primary hemopoietic progenitors. J. Immunol. *176*, 5267–5275.

De Smedt, M., Hoebeke, I., Reynvoet, K., Leclercq, G., and Plum, J. (2005). Different thresholds of Notch signaling bias human precursor cells toward B-, NK-, monocytic/dendritic-, or T-cell lineage in thymus microenvironment. Blood *106*, 3498–3506.

Debili, N., Coulombel, L., Croisille, L., Katz, A., Guichard, J., Breton-Gorius, J., and Vainchenker, W. (1996). Characterization of a bipotent erythro-megakaryocytic progenitor in human bone marrow. Blood *88*, 1284–1296.

Deng, W.M., Althauser, C., and Ruohola-Baker, H. (2001). Notch-Delta signaling induces a transition from mitotic cell cycle to endocycle in Drosophila follicle cells. Development *128*, 4737–4746.

Deveaux, S., Filipe, A., Lemarchandel, V., Ghysdael, J., Romeo, P.H., and Mignotte, V. (1996). Analysis of the thrombopoietin receptor (MPL) promoter implicates GATA and Ets proteins in the coregulation of megakaryocyte-specific genes. Blood *87*, 4678–4685.

Fang, T.C., Yashiro-Ohtani, Y., Del Bianco, C., Knoblock, D.M., Blacklow, S.C., and Pear, W.S. (2007). Notch directly regulates Gata3 expression during T helper 2 cell differentiation. Immunity *27*, 100–110.

Forsberg, E.C., Serwold, T., Kogan, S., Weissman, I.L., and Passegue, E. (2006). New evidence supporting megakaryocyte-erythrocyte potential of flk2/flt3+ multipotent hematopoietic progenitors. Cell *126*, 415–426.

Goldfarb, A.N. (2007). Transcriptional control of megakaryocyte development. Oncogene *26*, 6795–6802.

Hasserjian, R.P., Aster, J.C., Davi, F., Weinberg, D.S., and Sklar, J. (1996). Modulated expression of notch1 during thymocyte development. Blood *88*, 970–976.

Huang, E.Y., Gallegos, A.M., Richards, S.M., Lehar, S.M., and Bevan, M.J. (2003). Surface expression of Notch1 on thymocytes: correlation with the double-negative to double-positive transition. J. Immunol. *171*, 2296–2304.

Ishiko, E., Matsumura, I., Ezoe, S., Gale, K., Ishiko, J., Satoh, Y., Tanaka, H., Shibayama, H., Mizuki, M., Era, T., et al. (2005). Notch signals inhibit the development of erythroid/megakaryocytic cells by suppressing GATA-1 activity through the induction of HES1. J. Biol. Chem. *280*, 4929–4939.

Jarriault, S., Brou, C., Logeat, F., Schroeter, E.H., Kopan, R., and Israel, A. (1995). Signalling downstream of activated mammalian Notch. Nature *377*, 355–358.

Kaushansky, K. (2005). The molecular mechanisms that control thrombopoiesis. J. Clin. Invest. *115*, 3339–3347.

Kawamata, S., Du, C., Li, K., and Lavau, C. (2002). Overexpression of the Notch target genes Hes in vivo induces lymphoid and myeloid alterations. Oncogene *21*, 3855–3863.

Krivtsov, A.V., Twomey, D., Feng, Z., Stubbs, M.C., Wang, Y., Faber, J., Levine, J.E., Wang, J., Hahn, W.C., Gilliland, D.G., et al. (2006). Transformation from committed progenitor to leukaemia stem cell initiated by MLL-AF9. Nature *442*, 818–822.

Kumano, K., Chiba, S., Shimizu, K., Yamagata, T., Hosoya, N., Saito, T., Takahashi, T., Hamada, Y., and Hirai, H. (2001). Notch1 inhibits differentiation of hematopoietic cells by sustaining GATA-2 expression. Blood *98*, 3283–3289.

Lam, L.T., Ronchini, C., Norton, J., Capobianco, A.J., and Bresnick, E.H. (2000). Suppression of erythroid but not megakaryocytic differentiation of human K562 erythroleukemic cells by notch-1. J. Biol. Chem. *275*, 19676–19684.

Luc, S., Anderson, K., Kharazi, S., Buza-Vidas, N., Boiers, C., Jensen, C.T., Ma, Z., Wittmann, L., and Jacobsen, S.E. (2008). Down-regulation of Mpl marks the transition to lymphoid-primed multipotent progenitors with gradual loss of granulocyte-monocyte potential. Blood *111*, 3424–3434.

Maillard, I., Koch, U., Dumortier, A., Shestova, O., Xu, L., Sai, H., Pross, S.E., Aster, J.C., Bhandoola, A., Radtke, F., and Pear, W.S. (2008). Canonical notch signaling is dispensable for the maintenance of adult hematopoietic stem cells. Cell Stem Cell *2*, 356–366.

Mancini, S.J., Mantei, N., Dumortier, A., Suter, U., MacDonald, H.R., and Radtke, F. (2005). Jagged1-dependent Notch signaling is dispensable for hematopoietic stem cell self-renewal and differentiation. Blood *105*, 2340–2342.

Mandal, L., Banerjee, U., and Hartenstein, V. (2004). Evidence for a fruit fly hemangioblast and similarities between lymph-gland hematopoiesis in fruit fly and mammal aorta-gonadal-mesonephros mesoderm. Nat. Genet. *36*, 1019–1023.

Mercher, T., Wernig, G., Moore, S.A., Levine, R.L., Gu, T.L., Frohling, S., Cullen, D., Polakiewicz, R.D., Bernard, O.A., Boggon, T.J., et al. (2006). JAK2T875N is a novel activating mutation that results in myeloproliferative disease with features of megakaryoblastic leukemia in a murine bone marrow transplantation model. Blood *108*, 2770–2779.

Nam, Y., Sliz, P., Pear, W.S., Aster, J.C., and Blacklow, S.C. (2007). Cooperative assembly of higher-order Notch complexes functions as a switch to induce transcription. Proc. Natl. Acad. Sci. USA *104*, 2103–2108.

Nam, Y., Sliz, P., Song, L., Aster, J.C., and Blacklow, S.C. (2006). Structural basis for cooperativity in recruitment of MAML coactivators to Notch transcription complexes. Cell *124*, 973–983.

Nerlov, C., Querfurth, E., Kulessa, H., and Graf, T. (2000). GATA-1 interacts with the myeloid PU.1 transcription factor and represses PU.1-dependent transcription. Blood *95*, 2543–2551.

Pear, W.S., Aster, J.C., Scott, M.L., Hasserjian, R.P., Soffer, B., Sklar, J., and Baltimore, D. (1996). Exclusive development of T cell neoplasms in mice transplanted with bone marrow expressing activated Notch alleles. J. Exp. Med. *183*, 2283–2291.

Pronk, C.J., Rossi, D.J., Mansson, R., Attema, J.L., Norddahl, G.L., Chan, C.K., Sigvardsson, M., Weissman, I.L., and Bryder, D. (2007). Elucidation of the phenotypic, functional, and molecular topography of a myeloerythroid progenitor cell hierarchy. Cell Stem Cell *1*, 428–442.

Radtke, F., Wilson, A., and MacDonald, H.R. (2004a). Notch signaling in T- and B-cell development. Curr. Opin. Immunol. *16*, 174–179.

Radtke, F., Wilson, A., Mancini, S.J., and MacDonald, H.R. (2004b). Notch regulation of lymphocyte development and function. Nat. Immunol. *5*, 247–253.

Rekhtman, N., Radparvar, F., Evans, T., and Skoultchi, A.I. (1999). Direct interaction of hematopoietic transcription factors PU.1 and GATA-1: functional antagonism in erythroid cells. Genes Dev. *13*, 1398–1411.

Schmitt, T.M., de Pooter, R.F., Gronski, M.A., Cho, S.K., Ohashi, P.S., and Zuniga-Pflucker, J.C. (2004). Induction of T cell development and establishment of T cell competence from embryonic stem cells differentiated in vitro. Nat. Immunol. *5*, 410–417.

Schmitt, T.M., and Zuniga-Pflucker, J.C. (2002). Induction of T cell development from hematopoietic progenitor cells by delta-like-1 in vitro. Immunity *17*, 749–756.

Schroeter, E.H., Kisslinger, J.A., and Kopan, R. (1998). Notch-1 signalling requires ligand-induced proteolytic release of intracellular domain. Nature *393*, 382–386.

Shivdasani, R.A., Fujiwara, Y., McDevitt, M.A., and Orkin, S.H. (1997). A lineage-selective knockout establishes the critical role of transcription factor GATA-1 in megakaryocyte growth and platelet development. EMBO J. *16*, 3965–3973.

Stier, S., Cheng, T., Dombkowski, D., Carlesso, N., and Scadden, D.T. (2002). Notch1 activation increases hematopoietic stem cell self-renewal in vivo and favors lymphoid over myeloid lineage outcome. Blood *99*, 2369–2378.

Subramanian, A., Tamayo, P., Mootha, V.K., Mukherjee, S., Ebert, B.L., Gillette, M.A., Paulovich, A., Pomeroy, S.L., Golub, T.R., Lander, E.S., and Mesirov, J.P. (2005). Gene set enrichment analysis: a knowledge-based approach for interpreting genome-wide expression profiles. Proc. Natl. Acad. Sci. USA *102*, 15545–15550.

Tsang, A.P., Visvader, J.E., Turner, C.A., Fujiwara, Y., Yu, C., Weiss, M.J., Crossley, M., and Orkin, S.H. (1997). FOG, a multitype zinc finger protein, acts as a cofactor for transcription factor GATA-1 in erythroid and megakaryocytic differentiation. Cell *90*, 109–119.

Tu, L., Fang, T.C., Artis, D., Shestova, O., Pross, S.E., Maillard, I., and Pear, W.S. (2005). Notch signaling is an important regulator of type 2 immunity. J. Exp. Med. *202*, 1037–1042.

Visan, I., Yuan, J.S., Tan, J.B., Cretegny, K., and Guidos, C.J. (2006). Regulation of intrathymic T-cell development by Lunatic Fringe-Notch1 interactions. Immunol. Rev. *209*, 76–94.

Weng, A.P., Ferrando, A.A., Lee, W., Morris, J.P., 4th, Silverman, L.B., Sanchez-Irizarry, C., Blacklow, S.C., Look, A.T., and Aster, J.C. (2004). Activating mutations of NOTCH1 in human T cell acute lymphoblastic leukemia. Science *306*, 269–271.

Weng, A.P., Nam, Y., Wolfe, M.S., Pear, W.S., Griffin, J.D., Blacklow, S.C., and Aster, J.C. (2003). Growth suppression of pre-T acute lymphoblastic leukemia cells by inhibition of notch signaling. Mol. Cell. Biol. *23*, 655–664.

Wilson, A., and Radtke, F. (2006). Multiple functions of Notch signaling in self-renewing organs and cancer. FEBS Lett. *580*, 2860–2868.

Zhang, P., Behre, G., Pan, J., Iwama, A., Wara-Aswapati, N., Radomska, H.S., Auron, P.E., Tenen, D.G., and Sun, Z. (1999). Negative cross-talk between hematopoietic regulators: GATA proteins repress PU.1. Proc. Natl. Acad. Sci. USA *96*, 8705–8710.